CANARD/LEF DESIGN FOR A MULTI-MISSION FIGHTER AIRCRAFT

M. Shepshelovich, D.Aboudi, E. Baharav, B. Epstein, A Luntz

Israel Aircraft Industries Ltd.
Ben-Gurion Airport, Israel

ABSTRACT

Leading edge flap and canard aerodynamic reshaping for a multi-mission fighter aircraft (LAVI) are discussed. Design target was improving transonic sustained turn performance of nominal aircraft configuration without penalizing supersonic characteristics.

The paper presents basic design principles, describes the theoretical design cycle and the experimental testing of newly designed elements.

I. INTRODUCTION

Conflicting design requirements for multi-mission fighter aircraft are a major driver in the configuration aerodynamic shaping. Superior transonic maneuverability, rapid supersonic acceleration, low level penetration capability, maximum available lift, efficient cruise are the usually specified points in the flight envelope.

Contradicting demands in different flight regimes result inevitably in a subsonic - supersonic compromise that affects the whole aerodynamic design process.

Close-coupled wing-canard layout requires induced drag optimization as a design starting point. After wing-canard interaction is designed for minimum induced drag, incorporating the effect of the fuselage at a certain design point, the answer for off-design requirements is the concept of variable camber, mission adaptive wing and rotating canard.

Limitation of the conventional pitch control combined with lateral-directional stability problems at high angles of attack reduce the possibility to fully exploit the benefits of CCV concept at maneuver.

Thus, following lifting surfaces design for a compromised lift coefficient and specified stability, the final aerodynamic shaping of movable Leading-Edge Flap (LEF) and rotating canard for a high loading case is the first clue for aerodynamic perfection in the flight envelope.

Thus the aim of aerodynamic reshaping of nominally defined LEF and canard described in this paper is to enhance aircraft transonic maneuverably without penalizing supersonic performance.

II. BASIC MISSION ADAPTIVE WING

Since LEF-canard reshaping was performed relative to the nominal geometry, some of the aerodynamic features of this basic configuration are discussed in this section.

LAVI aircraft wing theoretical evaluation is described in detail in Refs. 1-3. General design considerations are summarized in this section.

Basic wing design point (C_L=0.2, M=0.9) was a matter of classical subsonic/supersonic compromise and was considered to be a starting point in the attempt to solve the principal conflict between performance considerations at transonic sustained turn (C_L=0.4-0.6, M=0.85) on the one hand and supersonic characteristics and performance at low level penetration mission on the other.(See Fig. 1).

It was intended to meet transonic maneuver requirements by downward deflection of the outboard leading-edge flap. At supersonic flight wing decambering by upward LEF deflection was planned to recover camber drag. (See Figs. 2-3 for schematic explanation). It was estimated (theoretically and experimentally) that up to 50% of drag penalties associated with high camber level may be recovered by wing decambering.

These features combined with rotating canard and downward elevon deflections for trimming unstable aircraft finalized the concept of mission adaptive wing (See Fig. 4).

It was believed at initial project stages that $C_{L_{DES}}$=0.2 may be regarded as an upper limit for basic wing design. Instability at transonic fight was derived from considerations of aircraft aft C.G. limit at subsonic high angles of attack and turned out to be relatively small. As a result, beneficial effect of high positive elevon defections was not exploited to the full extent at maneuver, justifying the above mentioned design upper limit.

Fig. 5 shows the schematic design flow chart. Wing-canard twist/camber were optimized for minimum induced drag for a specified pitching moment by the method described in Ref. 4.

Constraints imposed on aerodynamic design were as follow:

- nearly zero twist at wing root section
- straight elevon/LEF hinge lines
- ground clearance for weapon stations
- symmetrical canard

The wing was not constrained to have straight forming lines.

Recommended and adopted twist distributions relative to wind axis are shown in Fig. 6. Body angle of attack at design lift was chosen as α_B=3.2 deg. in order to provide required zero lift angle of attack.

Wing twist was defined around straight elevon hinge line. Twist distribution across the outboard wing also provided straight LEF hinge line. Resulting leading edge deviation relative to reference plane is shown in Fig. 7.

Maximum camber level adopted for baseline wing geometry is shown in Fig. 8.

Symmetrical canard was adopted for nominal aircraft configuration because of production considerations. It was planned to use canard rotation as a degree of freedom to minimize drag at different flight conditions. Tunnel testing indicated that proper canard scheduling versus angle of attack and Mach number contributes substantially to the drag minimization. However, it was understood that additional drag reduction may be realised only for cambered/twisted canard.

Parametric study of induced drag optimization at off-design lift coefficients indicated how canard should be scheduled versus angle of attack. It bacame clear (see Fig. 9) that canard should be set to a certain negative angle of attack at design list, its downward deflection being increased with angle of attacK.

There were also indications how wing geometry should be adjusted to off-design high lift case. Fig. 10 illustrates schematically that camber shapes recommended for medium lift coefficients may be simulated by downward deflections of LEF and elevons. There is an indication here how LEF should be scheduled versus angle of attack. It was also clear that realization of the recommended elevon downward deflection depends mainly on aircraft instability and aft C.G. limit considerations.

Experimental results showed good aerodynamic efficiency of the designed configuration. LEF and canard were optimally scheduled versus angle of attack and Mach number. LEF continuous downward deflection proved to be very effective and its contribution to lift at constant drag is shown in Fig. 11.

During the "LAVI" wing design stage, computer codes available at IAI were mainly linear potential panel methods (Refs. 4-6). Although their application in aerodynamic design procedure combined with intensive wind tunnel testing and a great deal of aerodynamic intuition provided impressive results, it was believed that aircraft lifting surfaces may be optimized more efficiently with the help of newly developed transonic analysis and design tools.

Suggestions to optimize LEF/canard came at relatively advanced project stages and were based on the following considerations:

- both parts were removable and their replacement did not required major aircraft redesign.
- fast development of transonic computational tools at IAI and accumulated experience in their practical applications to engineering problems increased the confidence in new design capabilities. Ref. 7-8 cover this subject.
- limitations of conventional pitch control at high angles of attack combined with lateral-directional stability problems lead to a situation that the beneficial effect of positively deflected elevons was not fully exploited at maneuver flight.
- it became evident, that adequate pitch control at high α is mandatory in order to support the combination of CCV concept with variable camber wing. Promising solutions, such as thrust vector control (2-D nozzles) or triple surface configuration were irrelevant for the LAVI project.
- LEF-canard optimization was a practical possibility to improve the lifting surfaces load carrying capability and to get a highly efficient drag polar for a relatively small instability level at transonic flight.

III. MODIFIED LEF AERODYNAMIC DESIGN

Modified leading-edge (L.E.) flap design illustrates the methodology developed as a part of thin wing design procedure. Design principles and theoretical results are presented in this section.

Theoretical analysis of nominal LEF indicated that there exists a certain potential for reducting transonic drag by fine L.E. shaping.

The aim of this work was to improve wing transonic performance by increasing leading-edge radius and slowing down the upper surface curvature decrease, thus lowering the suction peak and smoothing the stream velocity drop towards the trailing edge. As a result, L.E. flow separation may be delayed to a higher angle of attack and, in this way, an overall improvement in wing performance may be achieved (Ref. 9-10).

FL022IAI code was used for modified LEF design and performance evaluation. The body influence was not taken into account because of LEF outboard location. Since FL022IAI code is unable to treat two-surface problem (wing-canard), the wing only numerical model was run for all cases (exposed wing being extrapolated to the configuration center line).

The computations covered the lift coefficient range C_L=0.4=0.6 for M=0.85. New LEF performance was estimated relative to nominal wing both for deflected and undeflected flap positions.

A number of LEF's were constructed theoretically; some of them were identified as inferior during the evaluation program and were rejected prior to wind tunnel verification testing. H-FLAP, the most promising from a

theoretical point of view, underwent the tunnel evaluation program.

H-FLAP geometry at different span stations is shown in Fig. 12 relative to the nominal LEF. H-FLAP is characterized by 50% increase in LER and modified thickness distribution, which effects mainly the profile opening angle. L.E. droop, incorporated in H-FLAP, was increased gradually towards wing tip. Comparison of pressure distributions and calculated drag polar for undeflected flap case are given in Figs. 13-15.

However, the only correct way to estimate different L.E. flaps aerodynamic efficiency is to compare them when each one is deflected to its own optimal position. This type of comparison is presented in Fig. 16 in a cross-plotted form:

$\Delta C_D = C_D$ (DEFLECTED FLAP) - C_D (H-FLAP=0)

It may be seen that relatively small defections are required to set H-FLAP to its optimum position. By contrast, deflections of up to +13 deg. were estimated for the optimum setting of the nominal flap.

Performed calculations indicate that H-FLAP scheduling should be shifted by 9 deg relative to the nominal LEF. Pressure distribution comparison (H-FLAP versus nominal LEF; each one at its own scheduling) is given in Fig. 17.

Optimally scheduled H-FLAP indicates drag reduction of ≈20 cts relative to the nominal case at C_L=0.55, M=0.85. Translated to performance improvement, this gives lift gain $\Delta C_L/C_L$=1.5-2% at sustained turn. Local drag distribution across the span for wing with undeflected H-FLAP is shown in Fig. 18. Small flap deflections reduce the drag of outboard wing sections; However, it is clear that additional significant gain may come only with the incorporation of inboard L.E. flap.

Theoretically predicted improvement was a justification for a new LEF tunnel testing. For medium lift coefficients (C_L≈0.5 and higher) wind tunnel verification was especially needed because the flow in this case was not longer of a potential nature, at least at the wing tip. Theoretical drag prediction by potential codes is not so reliable here, which is even more true for off-design higher angles of attack.

Wing elastic deformation and its influence on drag at medium lift was checked at this stage. It was expected that an increase in elastic wing twist would result in reduced tip loading and improved drag characteristics. However, it was demonstrated (See Fig. 18), that a local lift decrease at outboard wing resulted in unfavorable drag redistribution, this nullifying the expected gains. Additional calculations indicated strongly that elasticity contributes to wing performance at higher angles of attack improving aircraft maximum turn capability.

IV. MODIFIED CANARD DESIGN

Design principles developed at the stage of LEF optimization were applied to the aerodynamic tailoring of twisted/cambered canard (Refs. 11-12).

Highly loaded canard was optimized for a minimum drag under the constraint of specified hinge and bending moments (defined actuators being the main consideration here).

Slight planform modification (SEE Fig. 19) was intended to decrease the neutral point arm relative to canard axis and, in this way, to compensate for the camber unfavorable effect on hinge moments.

Linear panel method (See Ref. 5) in design mode was used to construct canard twist (See Fig. 20). Design objectives were as follows:

- minimum supersonic wave drag
- constrained bending moment
- constrained hinge moment
- reduced tip loading

Maximum camber level adapted for initial canard iteration (CAN 4) was relatively low (see Fig. 21) and was increased significantly at advanced design stages (iterations CAN5-5, CAN5-15).

Theoretical estimations indicated that constraints on specified hinge and bending moments were met at all critical design points. Full configuration calculations were performed to confirm these facts (IAIFLO code - Ref. 6). It was shown that derivatives $C_{h\alpha}$ and $C_{h\delta CAN}$ decreased as a result of planform modification and compensated for the change of C_{ho} coefficient (see Fig. 22 for illustration).

The technique implemented for fine shaping of canard sections was the same as in H-FLAP design. However, rotating canard itself and its interference with body and wing was much more complicated than in the outboard LEF design. Transonic code for full configuration analysis (Refs. 13-14) was still under development.

To overcome these difficulties, MODCOM1 code (Ref. 15) for transonic wing analysis in presence of body was used as main design tool. Since wing upwash field was not accounted for in the MODCOM1 numerical model, full configuration analysis was completed with the help of IAIFLO code that was run at subsonic Mach number.

Typical pressure distributions for different canard iterations are shown in Fig. 23. The advantage of highly cambered canard is clearly seen.

Transonic potential codes used in the design procedure were unable to estimate characteristics of highly loaded symmetrical canard, which was also an indication that the case itself was too far from being a potential one. That is why most of the work on CAN5 aerodynamic shaping was performed relative to the iteration CAN4.

At that time CAN4 underwent tunnel testing and it was evaluated that it gives a lift gain of +1.5% relative to the nominal symmetrical

canard. This information provided an incentive to continue the work on CAN5 design.

MODCOM1 code calculations indicated that at lift coefficients of interest there is practically no difference between two iterations of CAN5 (See Fig. 24). Generally, a certain drag reduction was expected for newly designed canard. However, because of numerical model limitations it was hard to express this improvement in terms of aircraft characteristics.

Full configuration analysis at subsonic Mach numbers (IAIFLO panel code) indicated a lift gain of +1.0% for CAN5 relative to CAN4 case. Based on all these facts, a lift gain of +2.5% was predicted for CAN5 as compared to the configuration with symmetrical canard. It was clear also, that experimental verification for substantiating this prediction is needed here even more than in the case of H-FLAP design.

V. TRANSONIC EXPERIMENTAL VERIFICATION

Aerodynamic performance of newly designed elements was verified in transonic wind tunnel testing in the following stages:

Test NO. 1

H-FLAP + NOM.CAN. VS NOM.FLAP + NOM.CAN.

Test No. 2

CAN4 + NOM.LEF VS NOM.CAN + NOM.LEF
CAN4 + H-FLAP VS NOM.CAN + NOM.LEF

Test No. 3

CAN5 + NOM.LEF VS NOM.CAN + NOM.LEF
CAN5 + H-FLAP VS NOM.CAN + NOM.LEF

Test Mach numbers were
M=0.6, 0.85, 0.90, 0.95

The effect of newly designed elements on the aerodynamic performance was evaluated at different LEF-canard deflections. Final drag reduction was established for trimmed configuration at optimum LEF-canard scheduling.

H-FLAP performance is shown in Fig. 25 in terms of lift gains (at constant drag) relative to the nominal flap (LEF's scheduling used for these estimations is shown in Fig. 26). It was noted that flap efficiency depends slightly on canard deflection, which was attributed to canard upwash on outboard wing.

On average, lift gain of +2.0% was registered, which was fully consistent with theoretical predictions.

Comparison of theoretically predicted gains with experimental data is given in Fig. 27 and indicates very good agreement between them. Thus it was confirmed once more, that transonic potential codes when applied with some care to complicated engineering problems may become a very useful design tool even beyond strictly potential flow conditions.

At next experimental stage CAN4 performance was evaluated. Combined effect of H-FLAP and CAN4 was estimated also.

CAN4 transonic performance in terms of lift gains is shown in Fig. 28. To some suprise, it was discovered that canard efficiency was influenced by LEF deflections and when evaluated at optimum flap scheduling indicated smaller lift gains in comparison to configuration with undeflected LEF.

Combined effect of H-FALP + CAN4 on lift/drag characteristic is shown in Figs. 29-30. Canard deflections chosen for comparison gave nearly the same pitching moment characteristics and were close to optimum scheduling of each canard. Thus, non-trim data presented in Figs. 29-30 was very close to finally expected gains.

It was found, that for any practical purpose, H-FLAP and CAN4 contributions to overall aerodynamic performance were more or less additive. Lift gain of ≈+3.5% was estimated for combined LEF-canard effect which was equivalent to drag reduction of 6% at transonic sustained turn.

Lifting surfaces aerodynamic efficiency for improved configuration (non-trim data) was as following:

M = 0.85 C_L = 0.4 e = 0.90
C_L = 0.55 e = 0.83

It should be noted that additional significant improvement of aerodynamic efficiency may be achieved by incorporating wing inboard LEF into aerodynamic configuration.

Test data analysis for trimmed configuration did not change the preliminary estimated numbers. Finally calculated lift gains at trim for combined effect of H-FLAP and CAN4 are shown in Fig. 31 for optimally scheduled LEF and canard. Estimated drag reduction at different Mach numbers is given in Fig. 32.

Transonic test of configuration with CAN5 confirmed a lift gain of +1.0% relative to the CAN4 at M=0.85 and maneuver lift coefficients.

Combination of CAN5 and H-FLAP resulted in overall lift gain $\Delta C_L/C_L$=+4.5%, which is equivalent to 7-8% of drag reduction (See Figs. 31-32).

It should be noted that the improved configuration reduces drag up to relatively high lift coefficients. As a result, enhancement of maximum turn performance and, which is probably more important, improvement of aircraft take-off characteristics is expected.

VI. SUPERSONIC DECAMBERING EFFECT

The concept of wing supersonic decambering (Ref. 3) was evaluated theoretically and verified in wing tunnel testing at early project stages. For the nominal wing upward flap deflection δ_{LEF}=-4 deg. was adopted for small lift coefficients at supersonic and transonic low level penetration.

It was evident that for H-FLAP case highly drooped wing sections will require much larger decambering angle. It was not clear, however,

how much camber drag will be reduced in this extreme case.

Results of H-FLAP supersonic decambering test show that almost all camber drag of highly drooped wing section may be recover by relatively large upward LEF deflections. Decambering test results are presented in Figs. 33-34 in a cross plotted form.

$\Delta C_D = C_D(\text{H-FLAP}) - C_D\ (\text{NOM.LEF} = 0)$

Results of nominal wing decambering are shown also for comparison purpose.

Optimum decambering angle established for H-FLAP at supersonic was $\delta_{LEF} = -13$ deg.

It may be seen that at M=1.2 minimum drag level of decambered H-FLAP is similar or even slightly better as compared with decambered nominal wing. At M=1.75, a drag penalty of ≈5 cts was registered for H-FLAP.

Supersonic test results indicated also that there is practically no drag penalty for optimally scheduled CAN4 (low camber level). For highly cambered CAN5 a drag penalty close to 3 cts was evaluated.

VII. EULER CODE IMPACT ON AERO DESIGN

Transonic potential codes were used in this work as the main design and analysis tools. Evaluation of nonlinear aerodynamic charechateristics that were beyond the capabilities of potential methods was completed with the help of Euler code (wing only option).

Euler code capabilities to predict highly non-linear wing characteristics were evaluated at different stages of configuration improvement program. A matter of primary concern here was to find code's practical applications to every day engineering design problems.

Some results of this study are presented in this section. The stress was mainly on code capability to predict qualitative aerodynamic phenomena. However, in some cases very good agreement with experimental results was found (Ref. 16).

Fig. 35 illustrates code capability to predict maximum sectional lift at different span stations of nominal wing (undeflected L.E. flap). It should be noted that local lift of wing outboard sections shows practically linear characteristics up to $\alpha \approx 12\text{-}13$ deg. This linearity (although the flow here is of a vortical nature) is probably an explanation why potential code used beyond the boundaries of their applicability (α=10-11 deg.) still gave very reasonable results.

Local lift distribution across the span at different angles of attack is shown in Fig. 36. Flow breakdown on outboard wing and tip stall are clearly seen here.

Code application to the problem of L.E. flap hinge moments calculations is presented in Figs. 37-38 and shows very good agreement between calculated and tested characteristics. Reliable estimation of L.E. flap hinge moments was always beyond the capabilities of potential codes (the crucial point being prediction of maximum hinge moments).

Calculated wing pitching moment characteristics at high angels of attack with deflected and undeflected elevons are shown in Fig. 39. Wing stability and controllability characteristics were predicted here qualitatively up to high post-stall angles of attack.

Generally, it was concluded that Euler code application to aerodynamics of highly swept wings may widen significantly the engineering capabilities of design and analysis stages.

VIII. CONCLUSIONS

The redesign process described in the present paper is based on an extensive use of computational (mostly full potential) fluid dynamics codes and wind tunnel testing.

At the flight conditions in question, including the design point itself, the flow is not entirely potential. For this reason, the experimental verification of the gains, provided by the new configuration, became even more important.

The wind tunnel testing showed that the computational tools used, although applied far beyond their theoretical limitations, provided very good approximation to the experimental polars, up to angles of attack as high as 12°.

For moment prediction (including hinge moments), Euler codes had to be used.

At supersonic speed, a reliable drag evaluation of nonsmooth surfaces(wing with deflected flaps) was possible only through wind tunnel testing.

1. Geometrical reshaping of LEF and canard resulted in significant improvement of aircraft aerodynamic efficiency.

   Theoretically predicted lift gain of $\Delta C_L.C_L = +4.5\%$ ($M = 0.85$, $C_L = 0.55$) proved to be true at the stage of experimental verification. In drag terms it was equivalent to drag reduction of $\Delta C_D/C_D = 7 - 8\%$ over a wide range of lift coefficients. As a result, transonic sustained turn performance was improved by 0.6 deg/sec, which was the main target of aerodynamic design.

   Test results at transonic and subsonic Mach numbers indicated drag polars improvement up to relatively high lift coefficients. Based on these facts, it was concluded that enhancement of aircraft maximum turn characteristics and improvement of aircraft take-off performance are expected for modified configuration.

2. Combination of CCV flight control and concept of variable camber wing were employed to enhance maneuverability of unstable aircraft. However, limitations of conventional pitch control at high angles of attack impose severe constraint on allowable

instability, so that at transonic maneuver only some part of the beneficial effect of positive elevon deflections may be exploited.

Thus, high aerodynamic efficiency is required for non-trimmed configuration, the gains due to trim being an additional, but not the dominating factor.

A further efficiency improvement of non-trimmed aircraft at medium lift may be achieved by incorporation of wing inboard leading - edge flap into configuration.

However, it is clear that adequate pitch control at high α is mandatory in order to realize the full potential of variable camber wing over a wide range of lift coefficients.

3. Experimental evaluation of wing decambering concept at supersonic speeds indicated that most of the camber drag may be recovered by the relatively large LEF upward deflections.

Incorporation of highly dropped sections in a basic wing design penalize slightly performance only at maximum Mach numbers. This may be tolerable for aircraft whose primary role is air-to-ground attack mission.

In such circumstances, basic wing design point $C_{LDES} = 0.2$ can not be regraded any more as design upper limit. For highly drooped sections of variable camber wing it may be moved to higher lift coefficients.

LIST OF REFERENCES

1. Shepshelovich M., Rubin I., Robinson P.: "LAVI Wing Evaluation", IAI Report, 1982.

2. Shepshelovich M., "Elastic Tailoring for Lavi Wing" IAI report, 1982

3. Shepshelovich M.; "Wing Decambering", IAI Report, 1982

4. Lamar J.E., "A vortex lattice method for the mean camber shapes of trimmed non-coplanar planforms with minimum vortex drag", NASA TN D-8090.

5. Woodward F.A., "Analysis and Design of Wing-Body Combinations at Subsonic and Supersonic Speeds", Journal of Aircraft, Vol. V, NO. 6, Nov-Dec. 1968.

6. Jacobs A., "IAIFLO User Manual", IAI Report, 1979.

7. Luntz A., Epstein B., "Thin Delta Wing Transonic Computation", IAI Report, 1982.

8. Luntz A., Epstein B., Shepshelovich M., "LAVI Wings Transonic Computation", IAI Report, 1983

9. Epstein B., Luntz A., Shepshelovich M., "Modified LEF Evaluation" IAI Report,1983.

10. Shepshelovich M., "H-FLAP Aero Evaluation - Summary Report", IAI Report, 1984.

11. Bertochi R., Shepshelovich M., "Cambered Canard Aero Evaluation" IAI Report, 1986.

12. Baharav E., Aboudi D., Shepshelovich M., "Canard CAN5 Aero Evaluation", IAI Report, 1987

13. Luntz A., Epstein B., "A Multigrid Full Potential Transonic code for Arbitrary Configurations", GMD-Studien Nr.110, Proceedings of the 2nd European conference on MULTIGRID Methods, Koeln, 1985.

14. Epstein B., Luntz A.L., Nachshon A., "Multigrid Computation of Transonic Flow About Complex Aircraft Configurations, Using Cartesian Grids and Local Refinement" ICAS Proceedings, Jerusalem,Israel, Aug.1988.

15. Luntz A., "Transonic Small Disturbance Code for Body-Wing Configuration Coupled with Full Potential Code For Wing Alone". ICAS Proceedings, Seattle,W., Aug. 1982.

16. Bertochi R., Lubavin E., Shepshelovich M., "LEF Hinge Moments Estimation" IAI Report, 1986.

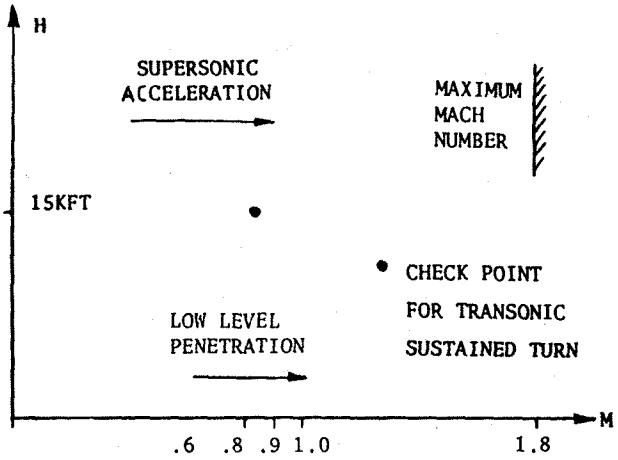

FIG 1. DESIGN POINTS DEFINITION

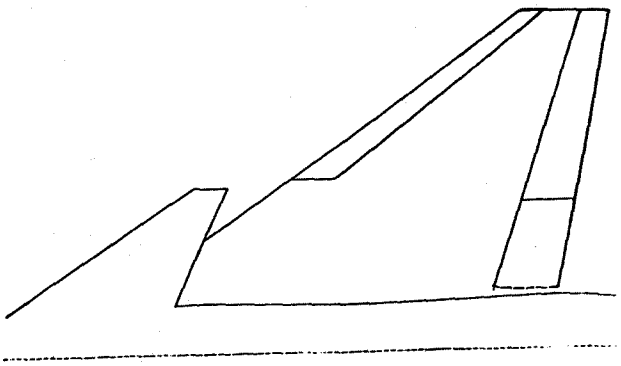

FIG 2. LAVI LIFTING SURFACES ARRANGEMENT

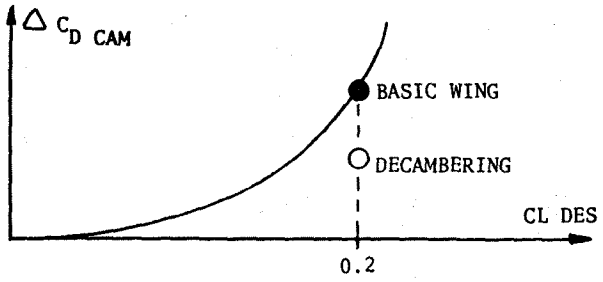

FIG 3. CAMBER DRAG RECOVERY

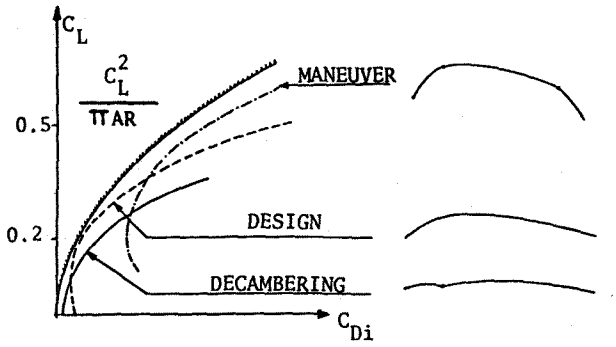

FIG 4. VARIABLE CAMBER WING CONCEPT

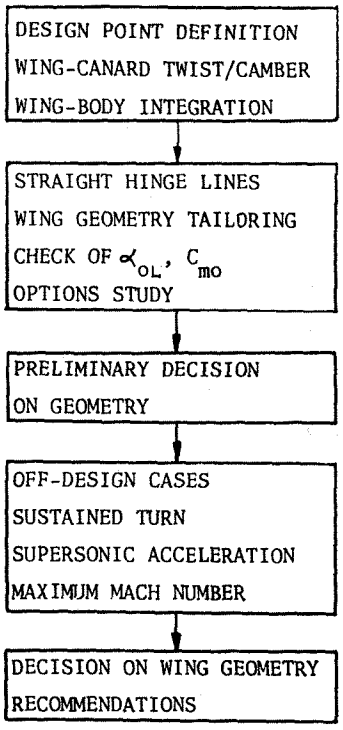

FIG 5. WING DESIGN FLOW CHART

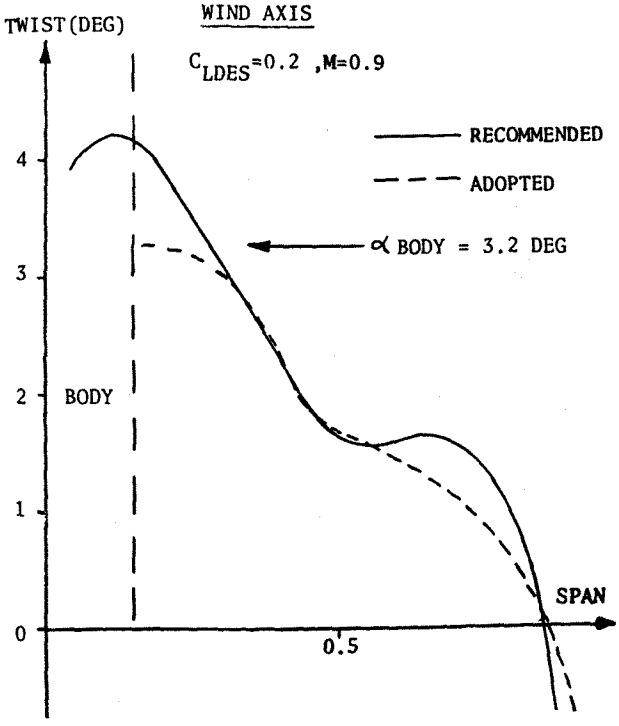

FIG 6. WING TWIST DISTRIBUTION

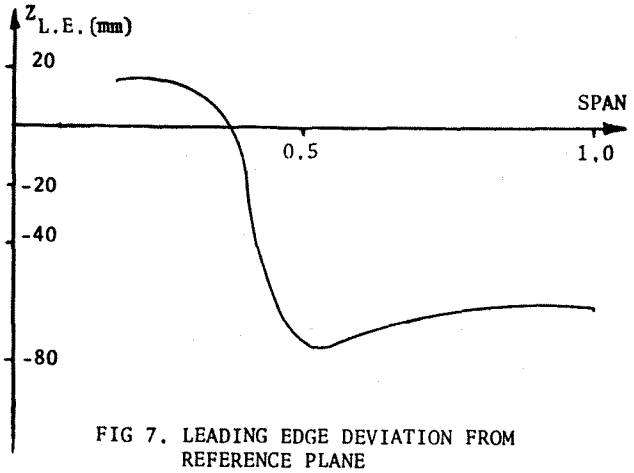

FIG 7. LEADING EDGE DEVIATION FROM REFERENCE PLANE

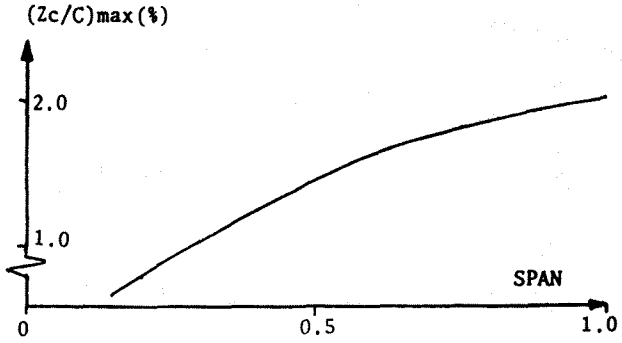

FIG 8. MAXIMUM CAMBER DISTRIBUTION

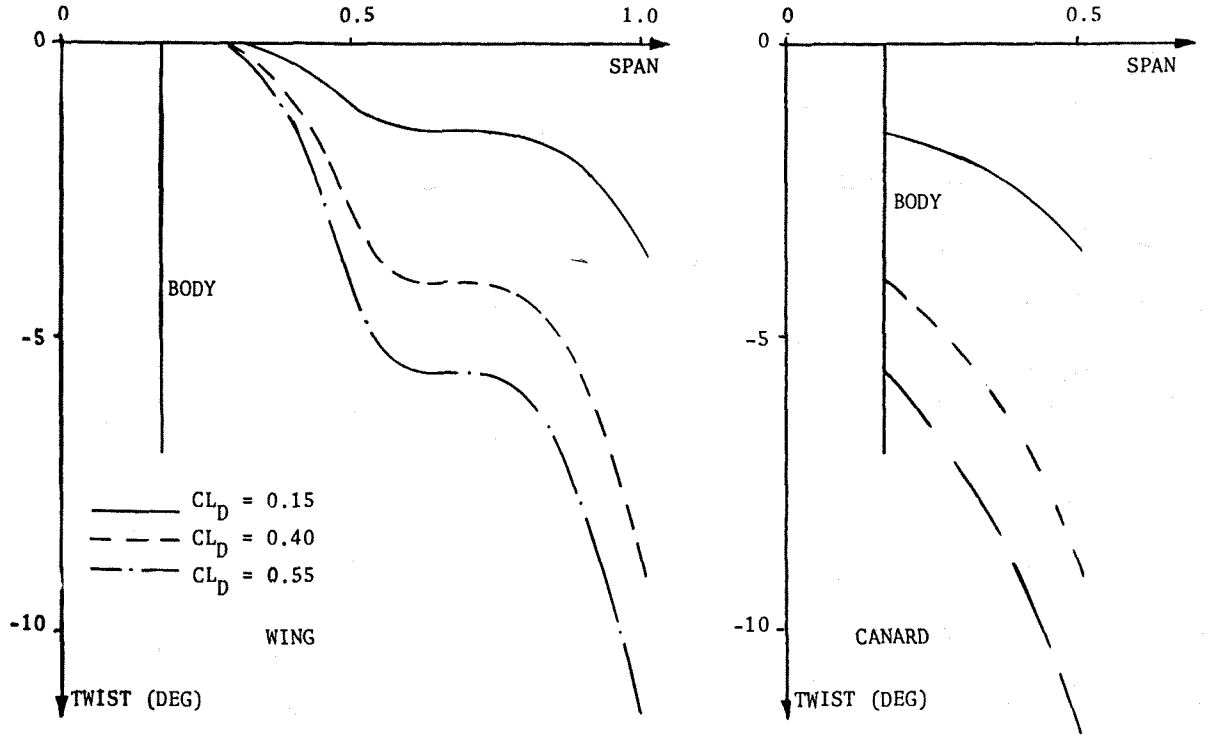

FIG 9. RECOMMENDED TWIST AS A FUNCTION OF DESIGN LIFT.

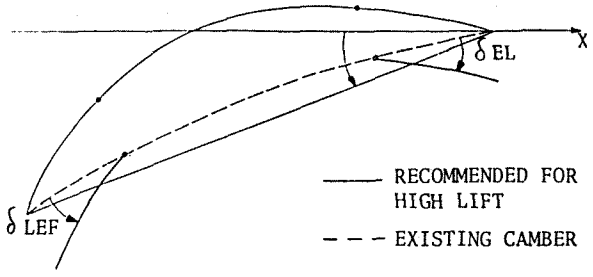

FIG 10. CAMBER SHAPE ADJUSTMENT TO HIGH LIFT COEFFICIENT

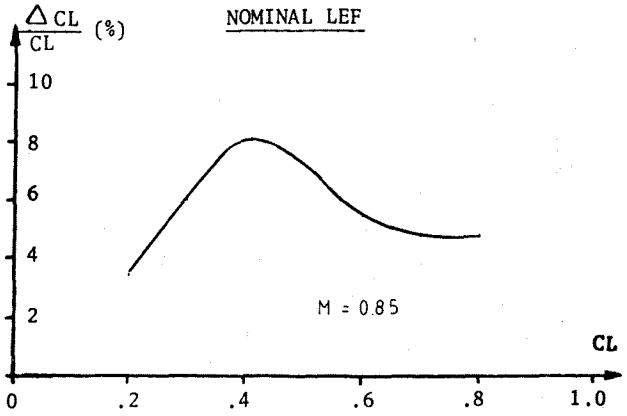

FIG 11. LIFT GAINS DUE TO LEF EFFECT

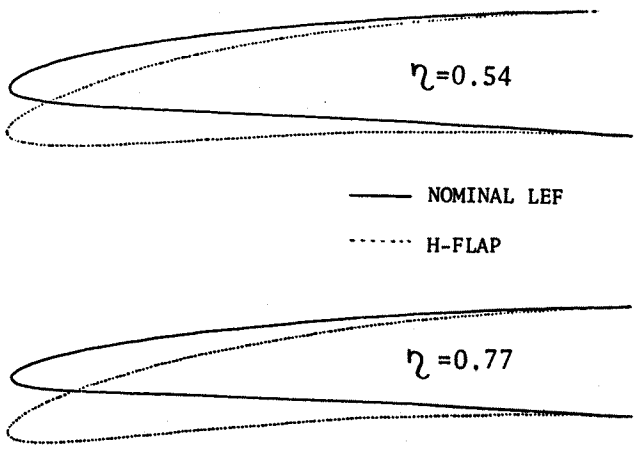

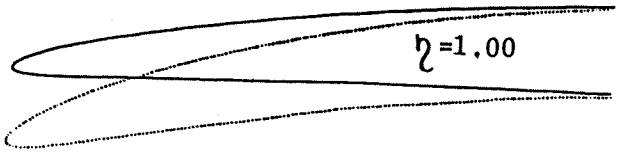

FIG 12. H-FLAP GEOMETRY VS NOMINAL LEF

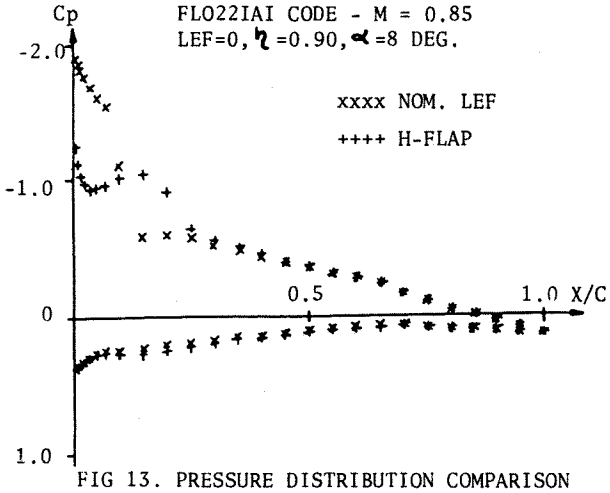

FIG 13. PRESSURE DISTRIBUTION COMPARISON

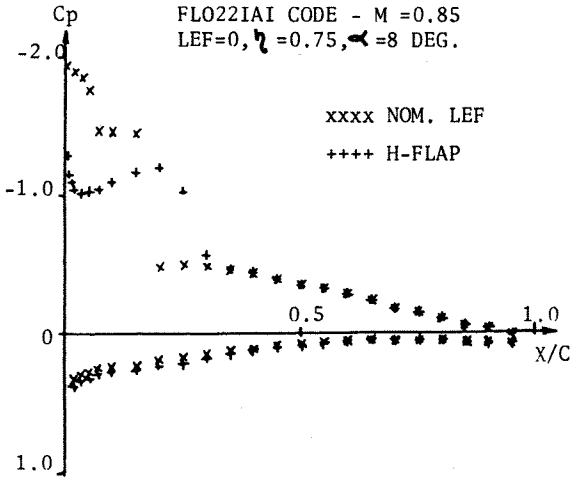

FIG 14. PRESSURE DISTRIBUTION COMPARISON

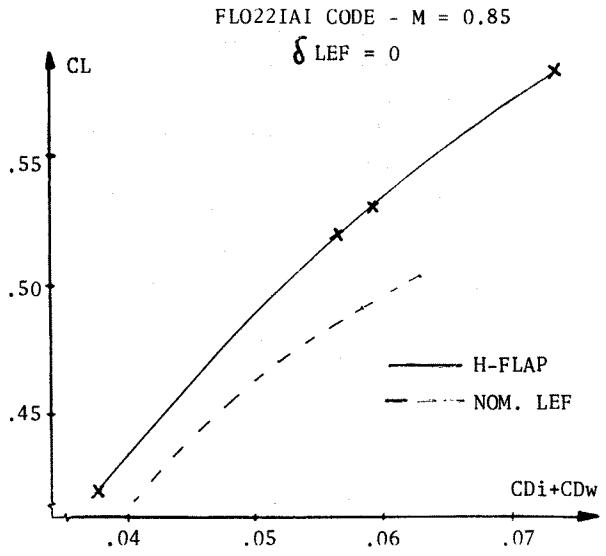

FIG 15. CALCULATED DRAG POLARS COMPARISON

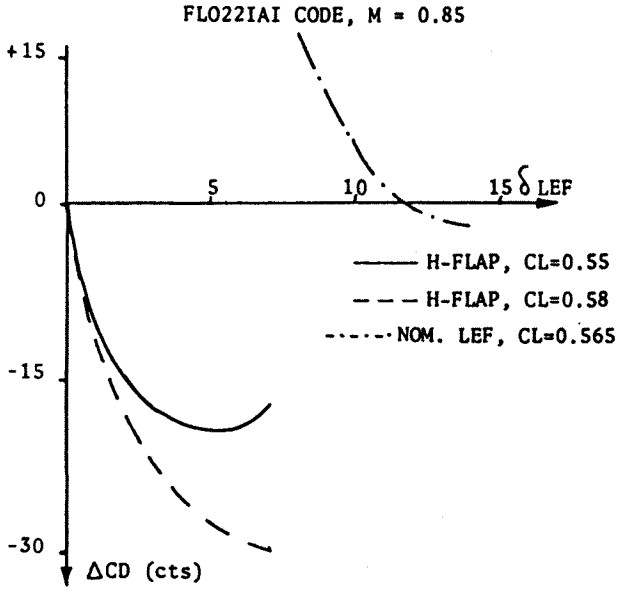

FIG 16. DRAG REDUCTION DUE TO H-FLAP EFFECT

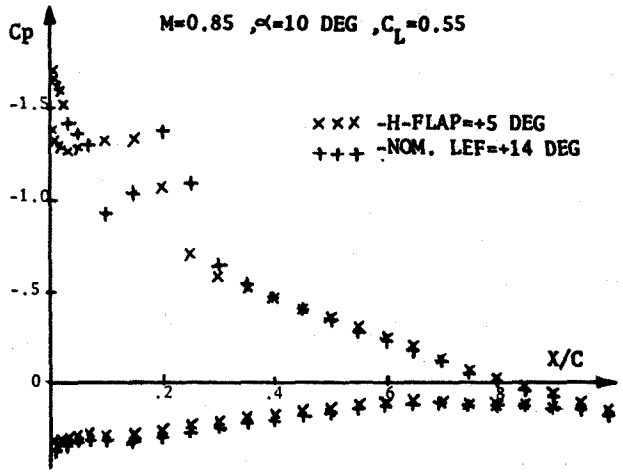

FIG 17. PRESSURE DISTRIBUTION COMPARISON

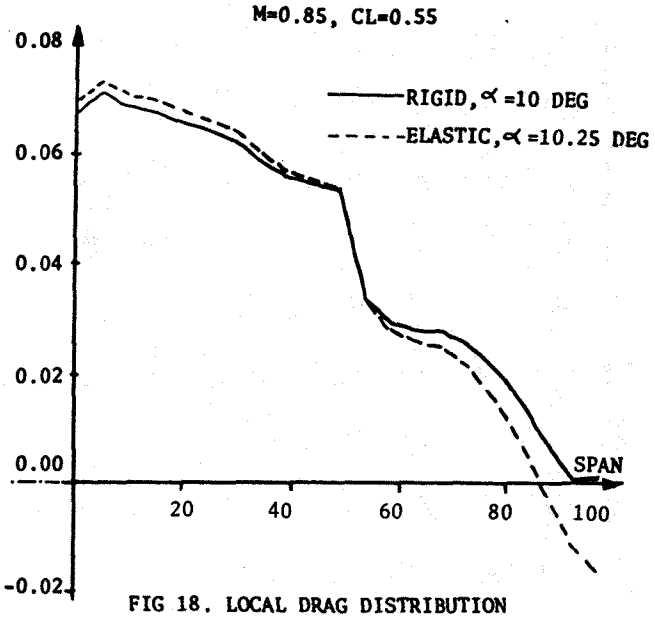

FIG 18. LOCAL DRAG DISTRIBUTION

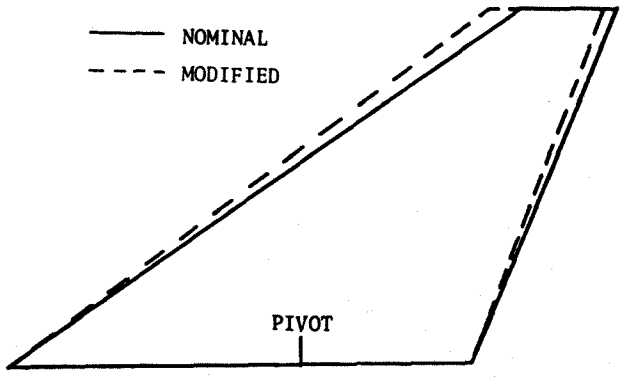

FIG 19. CANARD PLANFORM MODIFICATION

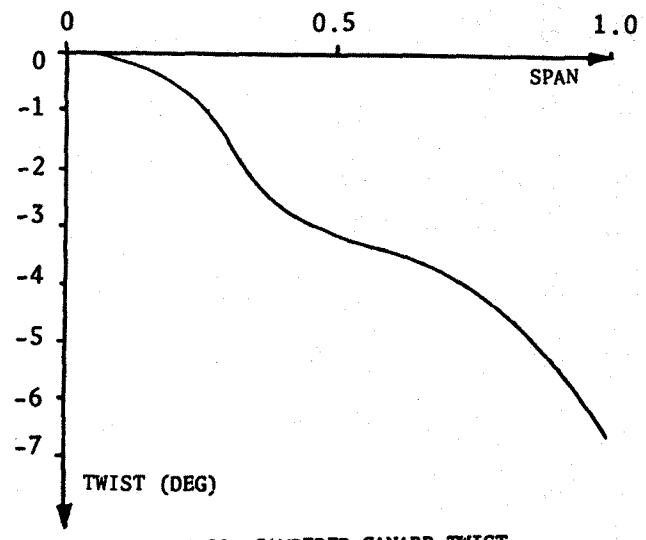

FIG 20. CAMBERED CANARD TWIST

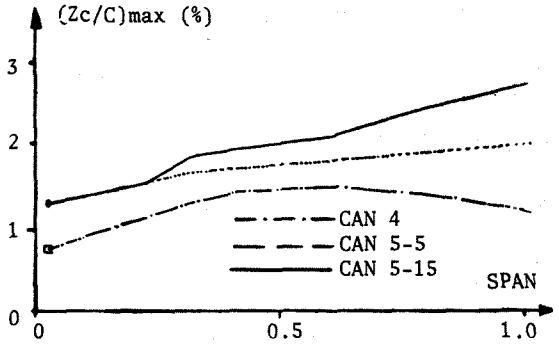

FIG 21. MAXIMUM CAMBER DISTRIBUTION

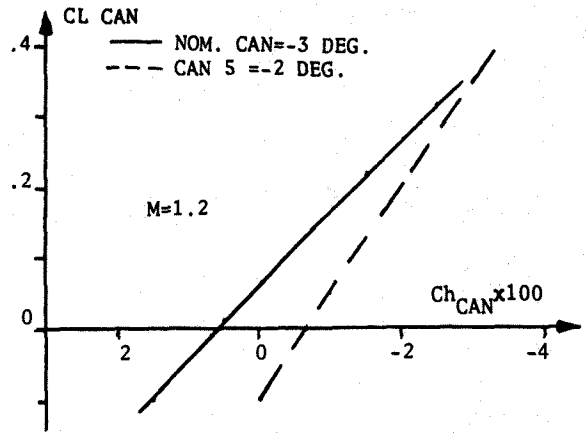

FIG 22. HINGE MOMENTS COMPARISON

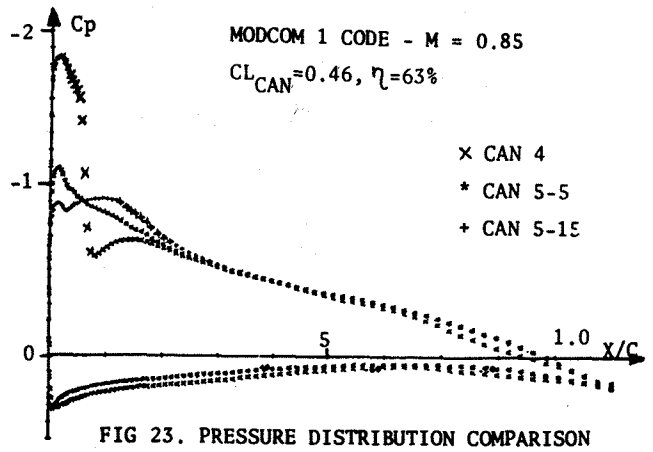

FIG 23. PRESSURE DISTRIBUTION COMPARISON

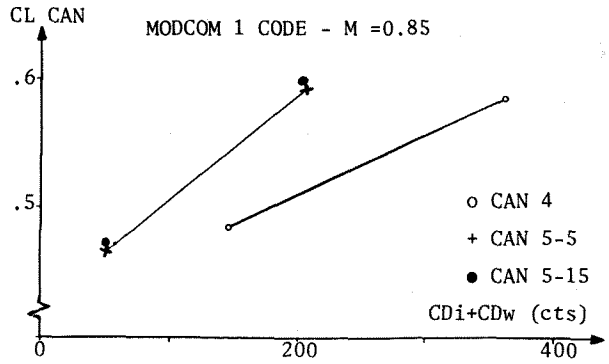

FIG 24. CAN 5 VERSUS CAN 4

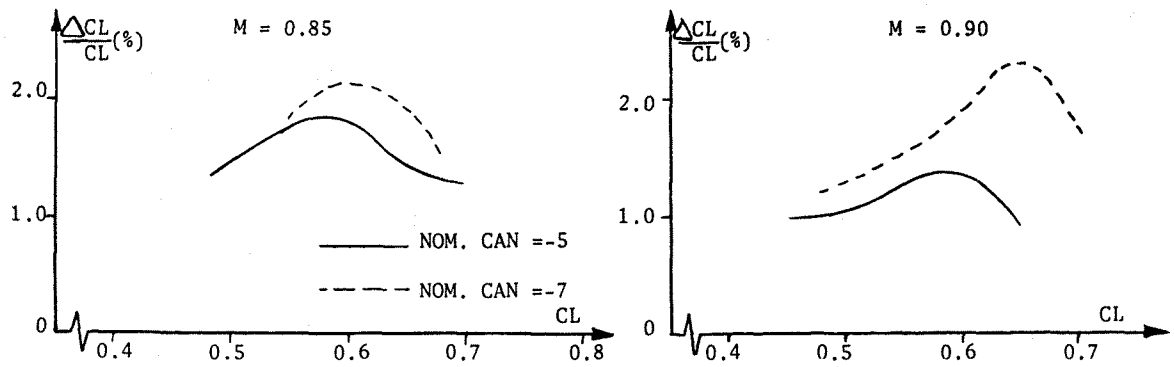

FIG 25. H - FLAP VERSUS NOMINAL WING

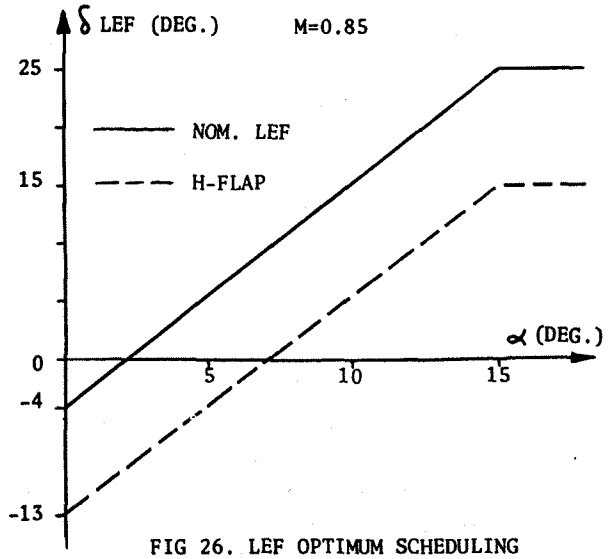

FIG 26. LEF OPTIMUM SCHEDULING

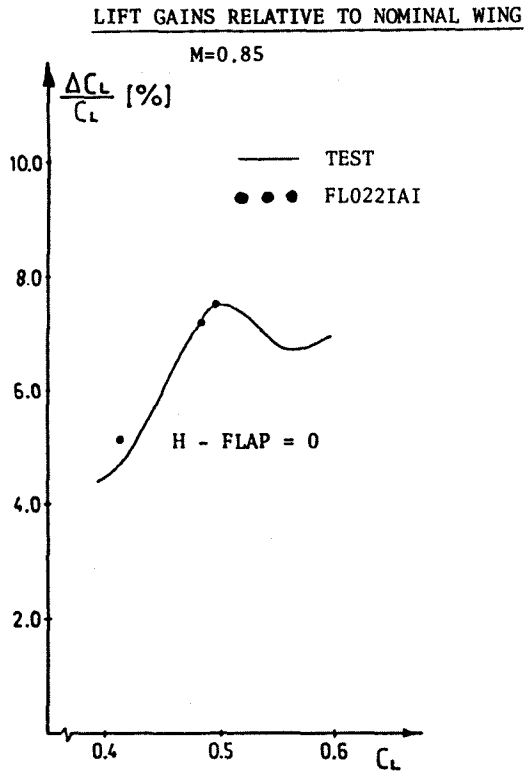

FIG 27A. THEORY - TEST COMPARISON

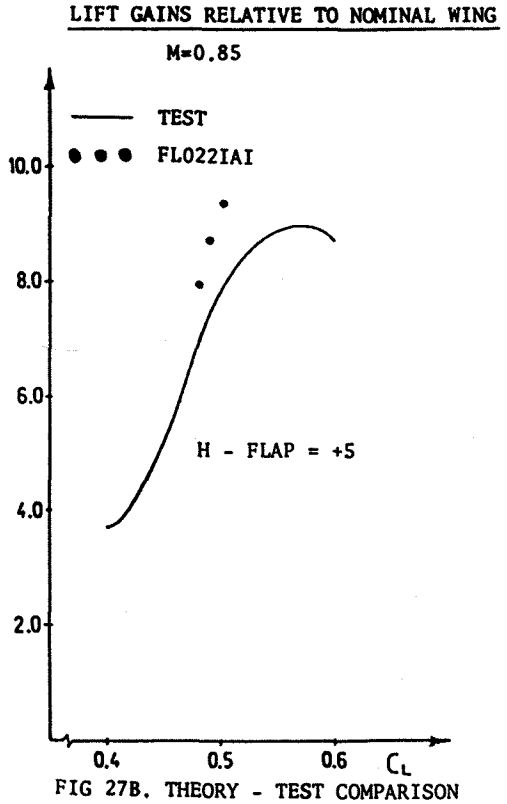

FIG 27B. THEORY - TEST COMPARISON

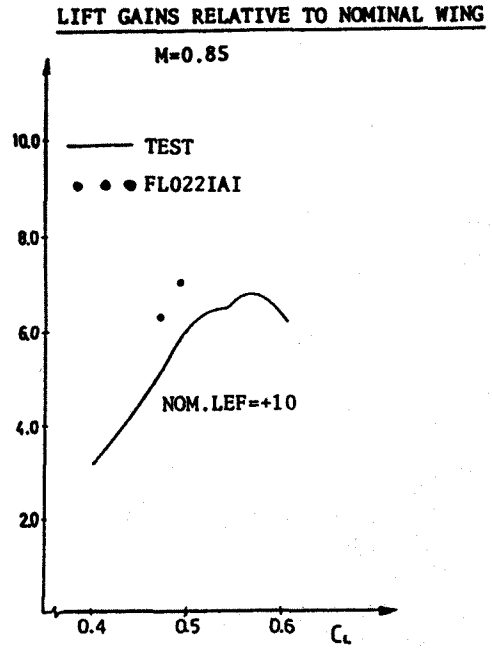

FIG 27C. THEORY - TEST COMPARISON

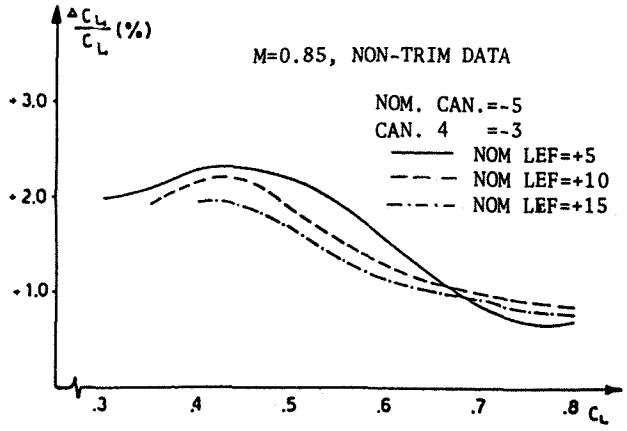

FIG 28. LIFT GAINS DUE TO CAN.4 EFFECT

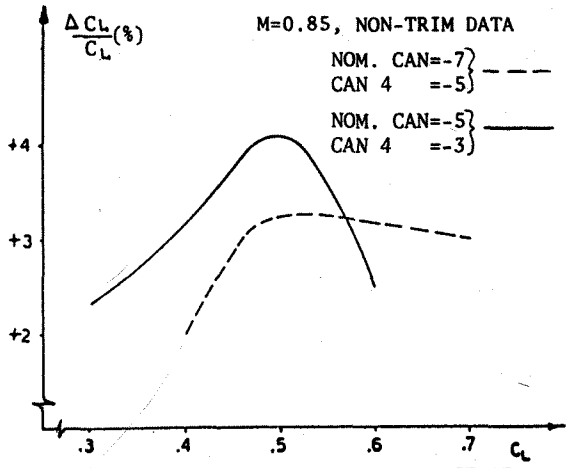

FIG 29. LIFT GAINS DUE TO EFFECT OF H-FLAP+CAN4

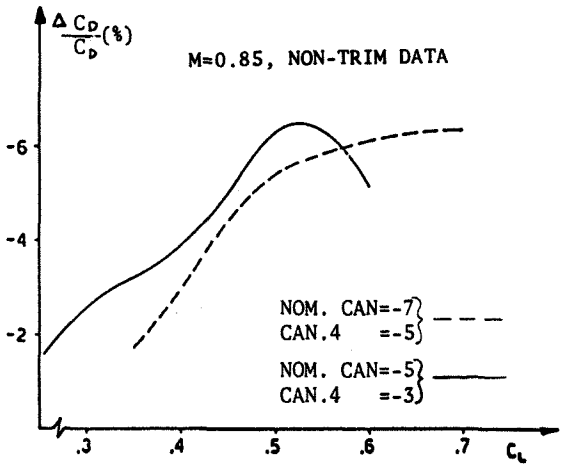

FIG 30. DRAG REDUCTION DUE TO EFFECT OF N-FLAP+CAN4

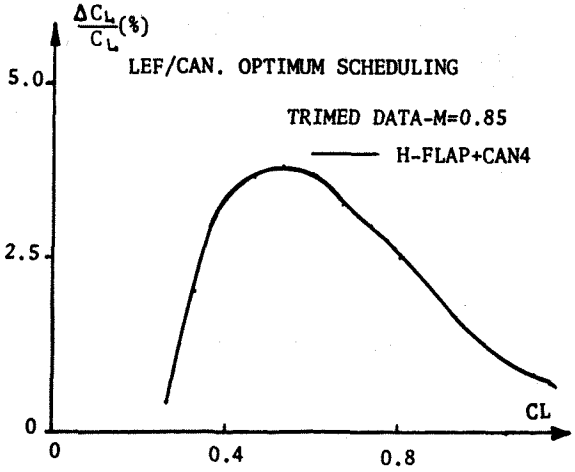

FIG 31. LIFT GAINS DUE TO H-FLAP+CAMBERED CANARD

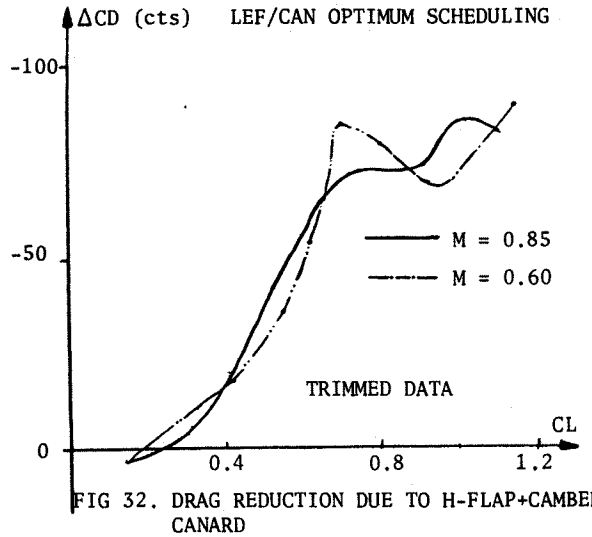

FIG 32. DRAG REDUCTION DUE TO H-FLAP+CAMBERED CANARD

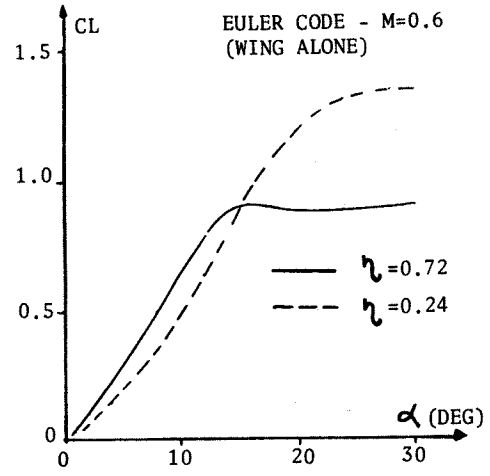

FIG 35. LOCAL LIFT AT HIGH ANGLES OF ATTACK

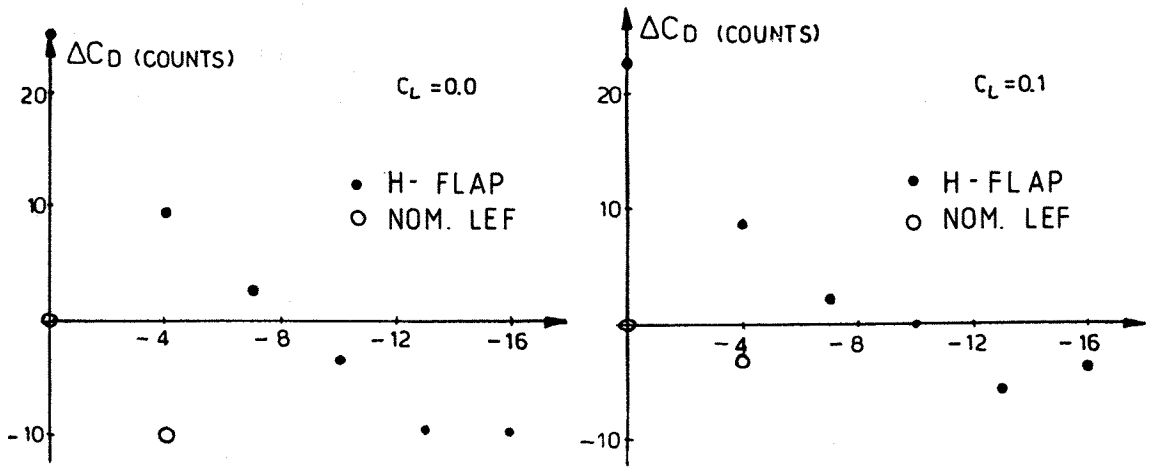

FIG 33. H - FLAP DECAMBERING - M =1.2

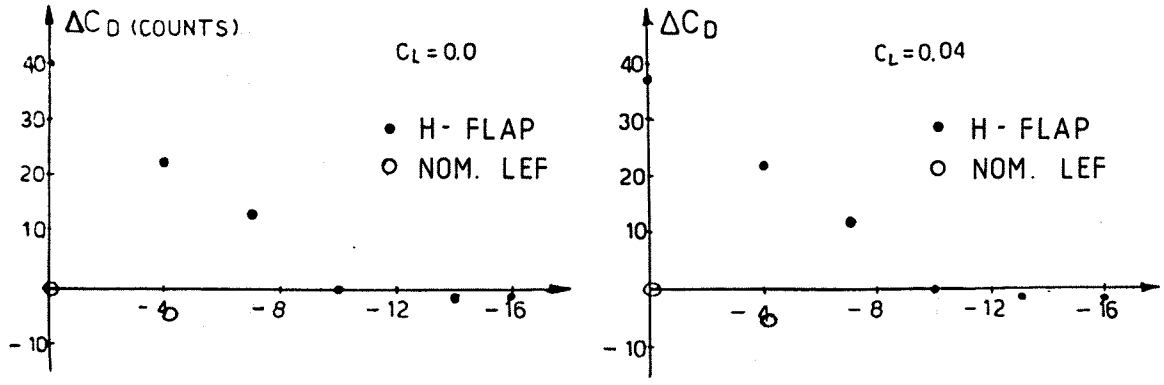

FIG 34. H - FLAP DECAMBERING - M = 1.75

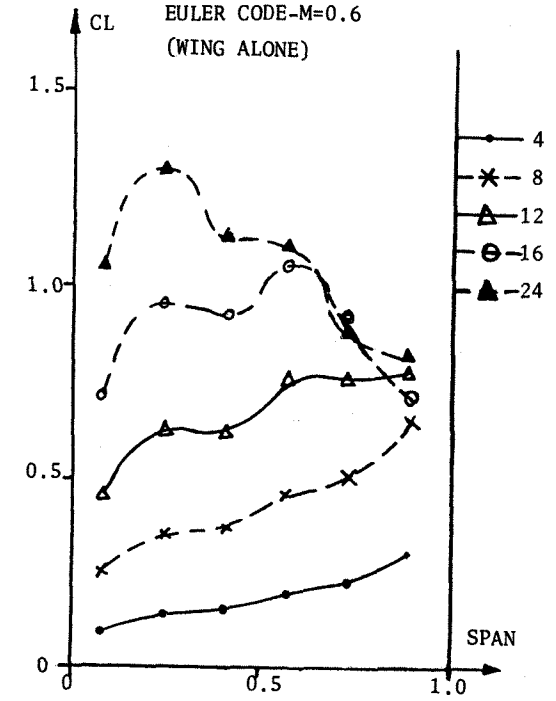

FIG 36. LOCAL LIFT DISTRIBUTION ACROSS THE SPAN

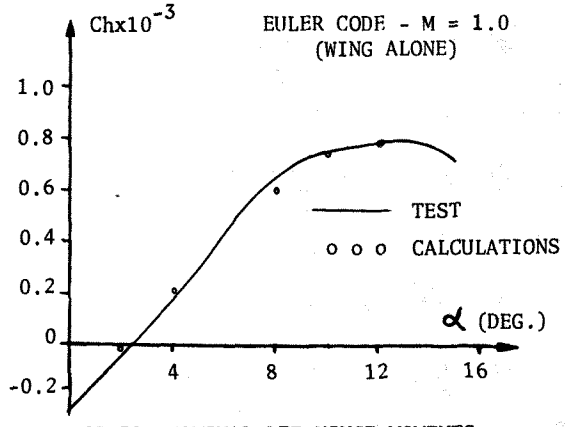

FIG 38. NOMINAL LEF HINGE MOMENTS

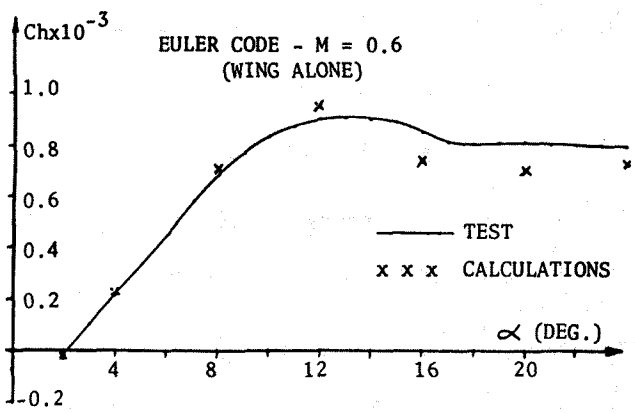

FIG 37. NOMINAL LEF HINGE MOMENTS

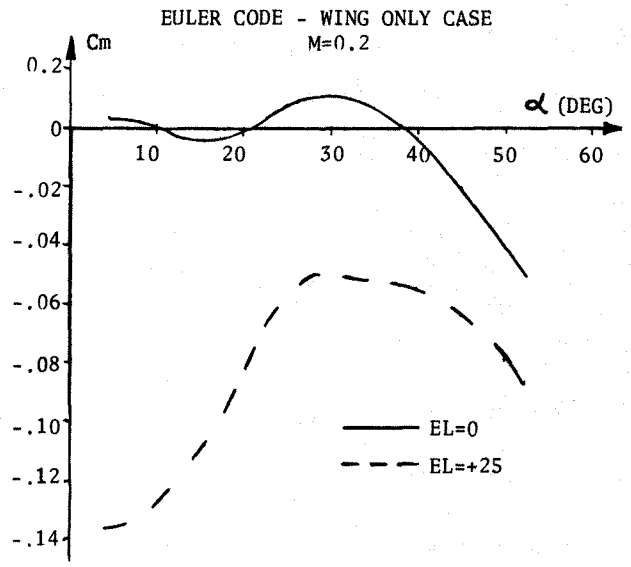

FIG 39. WING PITCHING MOMENT CHARACTERISTICS.